JOURNAL OF VIROLOGY, Jan. 1996, p. 415–426 Vol. 70, No. 1
0022-538X/96/$04.00+0


# Homologous RNA Recombination in Brome Mosaic Virus: AU-Rich Sequences Decrease the Accuracy of Crossovers

PETER D. NAGY AND JOZEF J. BUJARSKI*

*Plant Molecular Biology Center and the Department of Biological Sciences, Northern Illinois University, De Kalb, Illinois 60115*

Received 24 March 1995/Accepted 4 October 1995

**Brome mosaic virus, a tripartite positive-stranded RNA virus of plants, was used for the determination of sequence requirements of imprecise (aberrant) homologous recombination. A 23-nucleotide (nt) region that included a 6-nt UUAAAA sequence (designated the AU sequence) common between wild-type RNA2 and mutant RNA3 supported both precise and imprecise homologous recombination, though the latter occurred with lower frequency. Doubling the length of the 6-nt AU sequence in RNA3 increased the incidence of imprecise crossovers by nearly threefold. Duplication or triplication of the length of the AU sequence in both RNA2 and RNA3 further raised the frequency of imprecise crossovers. The majority of imprecise crosses were located within or close to the extended AU sequence. Imprecise recombinants contained either nucleotide substitutions, nontemplated nucleotides, small deletions, or small sequence duplications within the region of crossovers. Deletion of the AU sequence from the homologous region in RNA3 resulted in the accumulation of only precise homologous recombinants. Our results provide experimental evidence that AU sequences can facilitate the formation of imprecise homologous recombinants. The generation of small additions or deletions can be explained by a misannealing mechanism within the AU sequences, while replicase errors during RNA copying might explain the occurrence of nucleotide substitutions or nontemplated nucleotides.**

RNA-RNA recombination is important for increasing sequence variability among viral genomes and facilitating viral evolution (11, 15, 16, 29, 47, 57). It has been demonstrated experimentally in animal picornaviruses (22–25), coronaviruses (29, 33, 52), alphaviruses (53), orthomyxoviruses (6), and nodaviruses (31); in plant bromoviruses (4, 9, 10, 12, 18, 35–38, 42–44), carmoviruses (13, 14), tombusviruses (54, 55), tobamoviruses (5, 41), and alfalfa mosaic virus (50); and in bacteriophages (39, 40). These studies reveal three types of RNA recombinants, homologous, imprecise (aberrant) homologous, and nonhomologous (29), with homologous recombination the most frequent type (11, 24). During homologous events, no nucleotides are added, deleted, or modified in the crossover region compared with the parental sequences. Thus, the exact sites of crossovers are usually not known (except when marker mutations are present). Romanova et al. (45) and Tolskaya et al. (49) suggested that local heteroduplexes formed at regions of self-complementarity between two RNA templates could facilitate the generation of homologous recombinants in picornaviruses. Kuge et al. proposed that a supporting negative-sense RNA can bring the two parental positive-sense RNAs together (27). For coronaviruses, similar secondary structures between parental molecules have been proposed to facilitate homologous recombination (33). In a processive copy-choice model proposed for picornaviruses (22) and brome mosaic virus (BMV) (37), the 3′ end of the nascent strand (that is still part of the pausing replicase complex) anneals to complementary sequences on the acceptor strand and the replicase complex resumes RNA synthesis. None of these models have been experimentally confirmed.

Nonhomologous recombinants, which occur within nonsimilar sequence regions, were observed in tombusviruses (54, 55), carmoviruses (13, 14), nodaviruses (31), and bromoviruses (9, 10, 12, 18, 35–38) and in bacteriophage Qβ (8). The clustering of nonhomologous crossovers within or in the vicinity of local heteroduplexes between RNA templates was observed for BMV (36), while in turnip crinkle virus (TCV) the crosses were within one of three promoter-like motifs (13, 14).

Imprecise homologous recombinants were observed for BMV (37), cowpea chlorotic mottle virus (17), alphaviruses (53), and TCV satellite RNAs (13, 14). They have crossover sites flanked at least on one side by homologous sequences (29, 37) and sequence duplications, deletions, nucleotide substitutions, nontemplated nucleotides, or foreign sequences within the crossover region (29, 37). According to a model previously proposed by us (37), the nascent strand misanneals to the acceptor RNA before chain elongation is resumed by the replicase. Alternatively, Lai (29) assumes that the 3′ end of the nascent RNA strand misaligns to the acceptor strand because of the different RNA structures of the donor and acceptor sequences so the transcription complex resumes RNA synthesis from noncorresponding sequences.

The RNA components of BMV, a tripartite, single-stranded RNA virus of plants, contain approximately 200 nucleotides (nt) of homologous 3′ noncoding sequence (2). The 3′ portion of this region can form a tRNA-like conformation which is involved in the initiation of minus-strand synthesis (34). Most recombination experiments with BMV have utilized RNA3 mutants, since this RNA segment is dispensable for BMV RNA replication (1). Intersegment genetic recombination in BMV was observed in *Chenopodium hybridum* and *Chenopodium quinoa*, local lesion hosts for BMV (30, 35–38, 43, 44); barley, a systemic host (9, 35); and barley protoplasts (18, 35, 42).

Efficient homologous RNA recombination in BMV can be induced by 15- to 60-nt 3′ sequences that are homologous between RNA2 and RNA3 (37). Both the length and extent of sequence identity between the recombining RNAs were important. Some of the characterized homologous recombinants were imprecise. They contained single nucleotide substitutions (mismatches), nontemplated (additional) nucleotides, duplications, deletions, or insertions within the crossover region. It is likely that these sequence modifications delineate the actual

* Corresponding author.

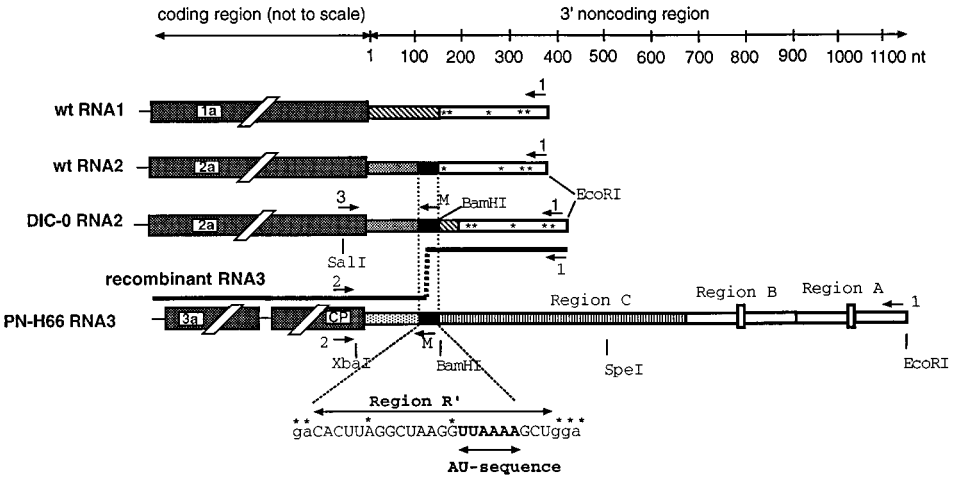


FIG. 1. Schematic representation of the 3′ noncoding regions of wt BMV RNA1, wt and DIC-0 RNA2s, and PN-H66 RNA3 constructs used for analysis of imprecise homologous recombination. The PN-H66 RNA3 mutant contains an ~1,250-nt chimeric 3′ noncoding region that consists of four elements (regions A to D). Region A contains wt RNA3 sequences located between positions 1 and 162 (counted from the 3′ end [2]) and an upstream RNA1-derived region (positions 163 to 236 in wt RNA1). Region B contains sequences located between positions 7 and 200 in wt RNA3. Regions A and B have a deletion (positions 80 to 100 in wt RNA3 [small rectangular boxes]). Region C has a 765-nt sequence derived from cowpea chlorotic mottle virus RNA3 (positions 24 to 788, counted from the 3′ end [3]). Region D (dotted box) contains wt RNA3 sequences located between positions 220 and 297. PN-H66 RNA3 also contains a 23-nt sequence (region R′ [positions 196 to 219 in wt RNA3, counted from the 3′ end]) that is identical to a corresponding region of wt and DIC-0 RNA2s (enclosed between dashed lines), except for the marker mutations indicated by asterisks. The locations of restriction sites are depicted by vertical lines, while the oligonucleotide primers used for PCR are shown by short horizontal arrows. Specifically, arrow M depicts the position of the following mutagenesis oligodeoxynucleotides: 2x1, 2x2, 3C, 3x, and 4x (see Materials and Methods).

crossover sites. The majority of these "fingerprints" concentrated at either of the two short AU-rich sequences of the region of homology.

To further study the mechanism of imprecise homologous recombination, in this work we investigated the role of a short AU-rich sequence (UUAAAA; called hereafter the AU sequence). The removal of the AU sequence decreased the occurrence of imprecise crossovers, whereas modifications of both the length and nucleotide order affected their incidence and/or the sites. We discuss our results in relation to mechanisms responsible for imprecise events.

## MATERIALS AND METHODS

**Materials.** Plasmids pB1TP3, pB2TP5, and pB3TP7 (21) were used to synthesize in vitro-transcribed wild-type (wt) BMV RNA components 1, 2, and 3, respectively. Plasmids PN-H66 and PN-H166 have been constructed previously (37). Moloney murine leukemia virus reverse transcriptase (RT) was from Gibco BRL (Gaithersburg, Md.); *Taq* DNA polymerase, restriction enzymes, and T7 RNA polymerase were from Promega Corp. (Madison, Wis.), and the Sequenase kit was from United States Biochemical Corp. (Cleveland, Ohio). The following oligonucleotide primers were used in this study (the unique *Eco*RI, *Hin*dIII, and *Bam*HI sites are underlined, mutated sequences are shown in bold letters, and alternative bases are shown in parentheses): 1, 5′-CAGTGAATTCTGG TCTCTTTTAGAGATTTACAG-3′; 2, 5′-CTGAAGCAGTGC-CTGCTAAG GCGGTC-3′; 3, 5′-AGAAGGTCGACGATTACGCTACC-3′; 2x1, 5′-CAGTG GATCCAAGCTTTT(AT)(AT)TTTTAAACTTAGCCAAAGTG-3′; 2x2, 5′-C AGTGGATCCAAGCTTTT(AT)A(AT)(AT)(AT)TAACCTTAGCCTAAGT G-3′; 3C, 5′-CAGTGGATCCAAGCTTTTAATTT(GT)GG(AC)CTTAGCC AAAGTG-3′; 3x, 5′-CAGTGGATCCAAGCTTTTAATTTTAATTT(AT)(AT) A(AC)CTTAGCCAAAGTG-3′; 4x, 5′-CAGTGGATCCAAGCTTTTAAA(A T)TTTTAAA(AT)TTTTAAA(AT)(AC)CTTAGCCAAAGTG-3′; 201, 5′-CAG TGGATCCAAGCTTTTAAAA**A**TTTGGGCCTTAGCC-3′; 202, 5′-CAGTGG ATCCAAGCTTTTAATTTGGGCCTTA**A**CC**TTT**GTGTCC-3′; 203, 5′-CAGT GGATCCAAGCTTTTAATTTGGGCCTTA**A**CCAAAGTGTCC-3′; 204, 3′-C AGTGGATCCAAGCTTTTAATTTTAATTTTTAAAAAAAAACCAAAGT GTCTTACC-3′; 236, 5′-CAGTAAGCTTGGATCCCTGTTCCAGGTAGGA AC-3′.

**Engineering of parental constructs.** The PN-MA plasmids described below are derivatives of pB3TP7, while the DIC plasmids are derivatives of pB2TP5. To obtain plasmids PN-MA2x-2, PN-MA2x-11, and PN-MA2x-13, a 196-bp 3′ cDNA fragment derived from PN-H66, a plasmid containing the full-length cDNA of BMV RNA3 with a modified 3′ end that includes a 6-nt AU sequence (UUAAAA) (37), was amplified out by PCR with primers 2 and 2x2 (Fig. 1). The amplified cDNA fragment was digested with *Bam*HI and *Xba*I and then used to replace the 3′ 166-bp *Bam*HI-*Xba*I fragment in PN-H66 (Fig. 1). The corresponding plasmids were selected by sequence analysis. A similar approach was used to generate the following constructs: PN-MA2x-C3 with primers 2 and 3C, PN-MA3x-57 with primers 2 and 3x, and PN-MA4x-11 with primers 2 and 4x.

To construct PN-MA2x-13NR, PN-MA2x-13 was digested with *Spe*I and *Eco*RI (Fig. 1) and the ends were filled in with T4 DNA polymerase. Subsequently, *Eco*RI linkers were added and the ends of the plasmid were religated.

To obtain the DIC-0 RNA2 construct, a 236-bp cDNA fragment representing the 3′ end of BMV RNA1 (including the conserved minus-strand initiation promoter [Fig. 1]) was amplified from pB1TP3 by PCR with primers 1 and 236. The resulting PCR product was digested with *Hin*dIII and *Eco*RI and then ligated between the corresponding sites in pB2SE, which carries the 500-bp *Sac*I-*Eco*RI region of pB2TP5 (21). Subsequently, the *Sac*I-*Eco*RI fragment of the resulting DIC-SacE plasmid was used to replace the corresponding fragment in pB2TP5. To construct plasmid DIC2x-10, a 201-bp 3′ cDNA fragment was obtained from pB2TP5 by PCR with primers 3 and 2x1 (Fig. 1). The amplified cDNA fragment was digested with *Bam*HI and *Stu*I and ligated between *Bam*HI and *Stu*I sites in DIC-0. A similar PCR-based approach was used to generate the following constructs: DIC2x-3, DIC2x-14, and DIC2x-16 with primers 3 and 2x2; DIC2x-C4 with primers 3 and C3; DIC3x-26 with primers 3 and 3x; and DIC4x-2 and DIC4x-6 with primers 3 and 4x. The entire PCR-amplified regions in all of the above constructs were sequenced to confirm the mutations introduced.

**Construction of full-length recombinant RNA3 clones.** Full-length cDNA clones of six types of precise and imprecise homologous recombinants (rec-4F1, rec-4F2, rec-4F5, rec-4F6, rec-4F7, and rec-6B2 [see Fig. 4F and 6B]) were constructed by transferring the fully sequenced *Bam*HI-*Xba*I inserts of each cloned 3′ recombinant RNA3 region into the corresponding positions of the full-length cDNA clone of PN-D (of which the entire 3′ noncoding region was sequenced [see below]). PN-D was obtained by replacing the 3′ *Hin*dIII-*Eco*RI fragment (positions 1 to 196 in wt RNA3 [as counted from the 3′ end]) of wt pB3TP7 with the corresponding fragment of DIC-0 described above. In addition, two of these reconstructed recombinants (rec-4F1 and rec-4F7) were also generated with recombinant DNA technology to make sure that the 3′ noncoding region is the only altered region in the entire recombinant RNA3 molecule. These constructs were named rec-4F1C and rec-4F7C (where C stays for cloning). Specifically, rec-4F1C was constructed by transferring the *Bam*HI-*Xba*I fragment of PN-MA3x-57 between these sites in PN-D. rec-4F7C was obtained by inserting the *Bam*HI-*Xba*I fragment of a PCR product obtained from construct PN-MA3x-57 with primers 2 and 204 into *Bam*HI-*Xba*I-digested PN-D. A similar PCR-based method was used to generate full-length clones of rec-6B201, rec-6B202, and rec-6B203 RNA3s with primer 2 and either primer 200, 201, or 202. A full-length cDNA clone of rec-4A2 was generated by replacing the wt 3′-terminal *Xba*I-*Eco*RI fragment of pB3TP7 with the corresponding *Xba*I-*Eco*RI fragment derived from the partial cDNA clone of rec-4A2 (see Fig. 4A).

**Barley protoplast and whole-plant inoculations.** Barley protoplasts were prepared (26) and inoculated (35) with different combinations of wt RNA1 and

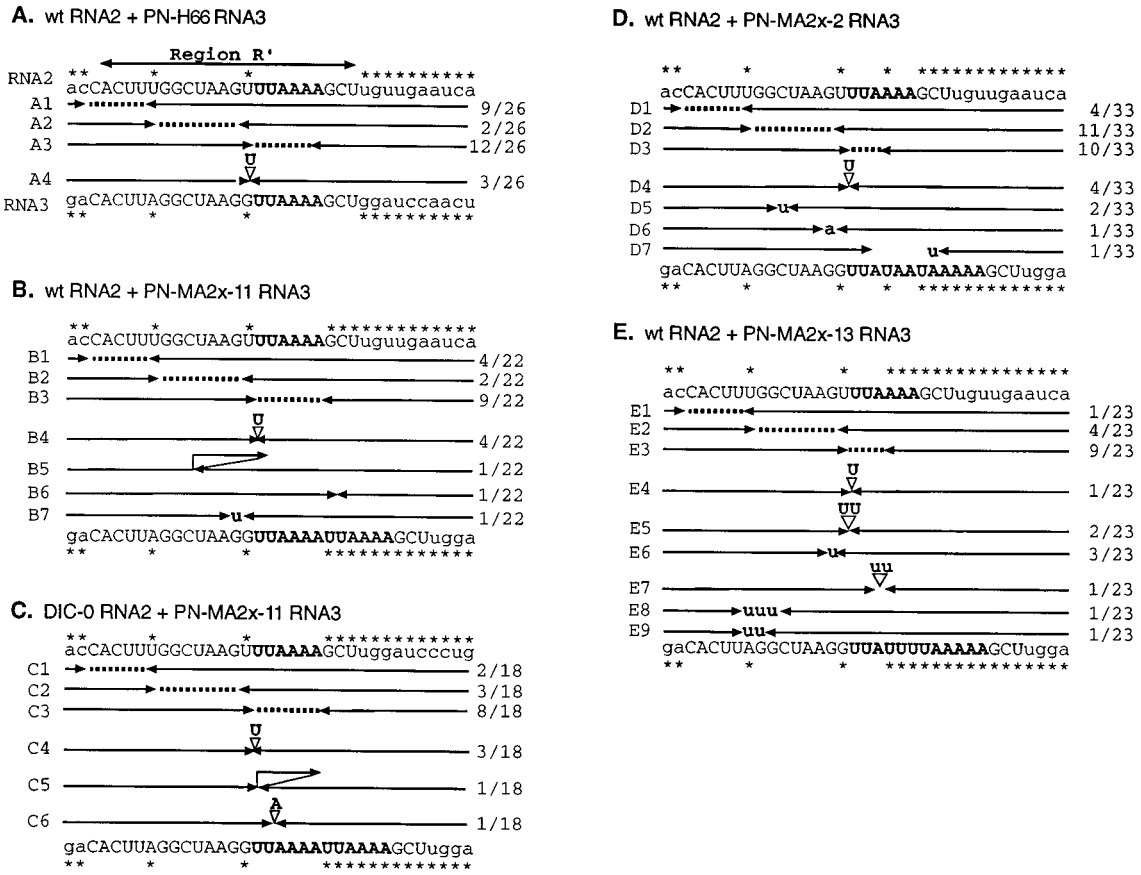


FIG. 2. Diagram summarizing the locations of crossover sites and modified nucleotides within the region R′ in the imprecise homologous RNA2/RNA3 recombinants isolated from infections with wt RNA1, wt and DIC-0 RNA2s, and RNA3 constructs (as shown) containing duplicated AU sequences. Homologous RNA2 and RNA3 positive-sense sequences are shown on the top and bottom lines, respectively. Capital letters depict the homologous region R′, whereas bold letters display AU sequences. Marker mutations within or adjacent to region R′ in RNA2 and RNA3 are indicated by asterisks. Each recombinant contains 3′-terminal sequences derived from RNA2 on the right side and 5′ sequences from RNA3 on the left side (Fig. 1). Each arrowhead below the sequence denotes the last nucleotide derived from RNA2, and each one above the sequence denotes the first nucleotide derived from RNA3. Dashed lines show ambiguous regions that could be derived from either RNA2 or RNA3 in precise homologous recombinants. Gaps between opposing arrowheads show deleted nucleotides, whereas sequence insertions are represented by open triangles. Capital letters mark possibly templated nucleotide insertions, while nontemplated nucleotides and nucleotide substitutions are shown by lowercase letters. Overlapping arrows show sequence duplications in imprecise recombinants. The nucleotide sequences in imprecise recombinants with ambiguous crossovers were arbitrarily placed with the upstream junction. Each RNA2/RNA3 recombinant was isolated from a separate local lesion. The incidence of each RNA3 recombinant and the total number of homologous recombinants are shown on the right.

mutants of RNA2 and RNA3. Total RNA was extracted as previously described (35) at 24 h postinoculation. One-fifth of the total RNA extract was separated by electrophoresis on a 1% agarose gel, transferred to a Hybond N+ (Amersham) nylon membrane, and hybridized to a $^{32}$P-radiolabeled probe specific for the BMV RNA-positive strand 3′ end, as described by Kroner et al. (26). In some experiments, barley protoplasts were inoculated with half of the total RNA extracts obtained from transcript-inoculated protoplasts as described previously (35).

Leaves of *C. quinoa* were inoculated with a mixture of transcribed BMV RNA components, as previously described by us (35). Briefly, a mixture of 1 μg of each transcript in 15 μl of inoculation buffer (10 mM Tris [pH 8.0], 1 mM EDTA, 0.1% celite, 0.1% bentonite) was used to inoculate one fully expanded leaf. Six leaves were inoculated for each RNA3 mutant. Each experiment was repeated twice.

**RT-PCR amplifications, cloning, and sequencing.** Total RNA was isolated from separate local lesions and used for RT-PCR amplification, exactly as described previously (35). The 3′ end of progeny RNA3 was amplified by using primers 1 and 2 (Fig. 1). Standard 1.5% agarose gel electrophoresis was used to estimate the sizes of cDNA products (46). cDNA fragments were digested with *Eco*RI-*Xba*I restriction enzymes and ligated between these sites into the pGEM-3Zf(−) cloning vector (Promega). The sites of crossovers were determined by sequencing with Sequenase according to the manufacturer's specifications (United States Biochemical Corp.).

**Analysis of the stabilities of AU sequences during infection.** The 3′ sequences of parental RNA2 constructs were amplified by RT-PCR with primers 1 and 3 from total RNA fractions extracted from separate local lesions on *C. quinoa* leaves 14 days after inoculation. Thereafter, amplified cDNA was digested with *Sal*I-*Eco*RI and ligated into the corresponding sites of pGEM-3Zf(−). The stabilities of AU sequences in the parental RNA3 and recombinant RNA3 (rec-4A2 [reconstructed as described above]) progeny were analyzed by RT-PCR, cloned, and sequenced, as described above for RNA3 recombinants.

## RESULTS

**Duplication of the AU sequence in RNA3 increases the frequency of imprecise homologous recombinants.** A previously engineered, BMV RNA3-based construct designated PN-H66 has a 23-nt insert (called region R′) that includes the AU sequence (Fig. 1). Region R′ is homologous to the corresponding region in wt RNA2. PN-H66 has been found to support homologous RNA2/RNA3 crosses in approximately 50% of local lesions on *C. quinoa* (37), with 11% of homologous recombinants found to be imprecise (Fig. 2A).

To test the importance of the AU sequence in imprecise homologous recombination, the AU sequence in PN-H66 was duplicated (Fig. 1). The resulting PN-MA2x-11 RNA3 was coinoculated with wt BMV RNA1 and RNA2 on *C. quinoa*. The accumulation of recombinants was monitored by RT-PCR

with primers 1 and 2 (Fig. 1), as described in Materials and Methods. On the basis of the lengths of amplified cDNA products, we estimated that 60% of local lesions contained wt-size RNA3 progeny, suggesting the accumulation of homologous recombinants. In these local lesions, the recombinant RNA3 completely outgrew PN-MA2x-11 parental RNA3 molecules, demonstrating their superior competitiveness over the 3′-modified parental RNA3s (35–38).

The sequencing of cloned RT-PCR products revealed that 32% of homologous recombinants were imprecise (Fig. 2B), a threefold increase over the unmodified R′ region. Two other RNA3 constructs (PN-MA2x-2 and PN-MA2x-13) that had A or U marker mutations within their duplicated AU sequences generated 24 and 36%, imprecise recombinants, respectively (Fig. 2D and E). The majority of these imprecise variants contained one or two nucleotide changes (insertions or substitutions) within the AU sequence or within an upstream UAAGU/G region (Fig. 2B, D, and E).

Control RT-PCR amplifications of mixtures of in vitro-transcribed wt RNA1s and RNA2s and PN-MA2x-11 RNA3 generated parental-size, but not recombinant-size, RNA3-specific cDNA fragments (data not shown). Similar controls were published previously (35–38); they exclude the possibility that the recombinants represent RT-PCR artifacts.

**Expanding the AU sequences in both RNA2 and RNA3 components further increases the frequency of imprecise crosses.** In order to facilitate in vitro mutagenesis of the AU sequence in the region R′ of RNA2, a construct designated DIC-0 (Fig. 1) was generated. In DIC-0, the 3′-terminal 196 nt have been replaced with the 3′-terminal 236 nt of wt RNA1 so that region R′ is separated from the 3′-terminal negative-strand initiation promoter. This and an engineered unique *Bam*HI site (Fig. 1) allowed further modifications of the internal AU sequences without affecting in vivo accumulation. DIC-0 RNA2 and its derivatives (DIC2x-10 and DIC2x-16) were coinoculated with wt RNA1 and PN-MA2x-11 (Fig. 2B) or rec-4A2 RNA3 constructs on barley protoplasts or *C. quinoa* plants. rec-4A2, a recombinant RNA3 obtained during this work (see Fig. 4A), contains a duplicated AU sequence in region R′, and it has a 3′ noncoding region identical to that of DIC-0 RNA2. Northern (RNA) blot analysis (Fig. 3) demonstrates that the accumulations of DIC-0, DIC2x-10, and DIC2x-16 RNA2s in barley protoplasts and *C. quinoa* plants were comparable. Thus, modifications in the AU sequence of region R′ did not significantly influence the level of RNA2 templates available for recombination. In addition, Fig. 3B shows that despite extended 3′-terminal sequences, rec-4A2 RNA3 replicated efficiently in local lesions.

To compare the recombination activity of DIC-0 RNA2 with that of wt RNA2, either DIC-0 RNA2 or wt RNA2 was coinoculated with wt RNA1 and PN-MA2x-11 RNA3. This demonstrated that the R′ regions of DIC-0 and wt RNA2s generated similar levels of both precise and imprecise homologous recombinants with PN-MA2x-11 (Fig. 2B and C), accumulating imprecise recombinants in 28 and 32% of local lesions, respectively. Besides showing the high recombination activity of DIC-0 RNA2, this observation reveals that sequences 3′ to the AU sequence in RNA2 do not significantly influence imprecise homologous recombination.

To examine the effects of AU sequence duplication in two recombining RNA molecules, DIC2x-10 RNA2 was coinoculated with wt RNA1 and PN-MA2x-11 RNA3. The accumulating homologous RNA3 recombinants were cloned and sequenced. Figure 4A shows that the fraction of imprecise homologous recombinants increased to 54%. Interestingly, the majority (58%) of these imprecise recombinants had nucleotide substitutions, while the rest had either nontemplated nucleotides or sequence deletions (e.g., rec-4A6 and rec-4A7 [Fig. 4A]). This profile differs from that found when RNA3 was the only component with a duplicated AU sequence.

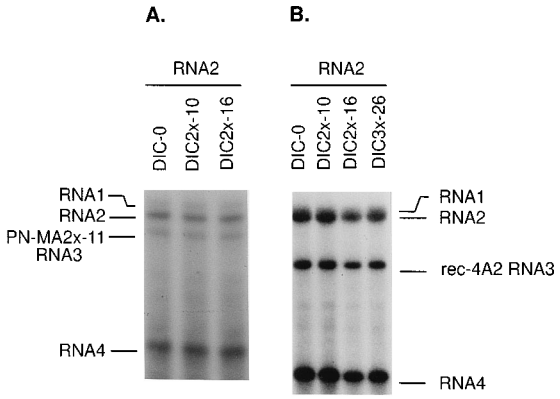


FIG. 3. Analysis of the accumulation levels of various parental RNA2 mutants in barley protoplasts and whole plants, as determined by Northern blotting. Barley protoplasts and *C. quinoa* leaves were inoculated with a mixture of in vitro-transcribed wt RNA1, the RNA2 variant shown above each lane, and either PN-MA2x-11 or rec-4A2 RNA3. rec-4A2 RNA3 is a reconstructed RNA2/RNA3 recombinant (see Fig. 4A). Barley protoplasts and *C. quinoa* plants were incubated for 24 h and 2 weeks, respectively. Total RNA extracts were isolated and separated by electrophoresis on a 1% agarose gel. RNA was transferred to a nylon membrane and probed with a 200-nt $^{32}$P-labeled RNA probe specific for the 3′ noncoding region of RNA1 to RNA4, as described in Materials and Methods. (A) Accumulation levels of parental RNA2s and PN-MA2x-11 RNA3 in barley protoplasts; (B) accumulations of rec-4A2 RNA3 in the presence of the indicated RNA2s in *C. quinoa* plants.

To map the crossover sites more closely, A or U marker modifications were introduced into the AU sequence of DIC2x-10 RNA2. The resulting DIC2x-3 and DIC2x-16 RNA2s (Fig. 4B to E) were coinoculated with either PN-MA2x-11 RNA3 or one of its mismatch derivatives (PN-MA2x-2 or PN-MA2x-13). As seen in Fig. 4B to E, 52% of the 77 separate homologous recombinants tested were imprecise and 74% of the imprecise recombinants had sequence substitutions. In all but one (rec-4C6 [Fig. 4C]), the nucleotide substitutions were located within a region flanked by RNA2 and RNA3 marker mutations, supporting the conclusion that they point to the actual crossover sites. The RNA2 and RNA3 variants carrying triplicated AU sequences, constructs DIC3x-26 and PN-MA3x-57, respectively, are shown in Fig. 4F. Coinoculated with wt RNA1, these molecules generated imprecise homologous recombinants even more frequently (61% [Fig. 4F] compared with 52% [Fig. 4A]). Interestingly, one recombinant (rec-4F10 [Fig. 4F]) contained as many as 15 nontemplated U residues at the crossover site. Approximately 60% of the imprecise junctions shown in Fig. 2A to E and 4A map at or close to the G marker mutation located just upstream from the AU sequence in RNA3. This marker mutation, however, is not responsible for the imprecise events since moving the marker(s) to other positions, for example, in DIC2x-2 and DIC2x-16 RNA2s yielded imprecise junctions frequently at the hot spot position just 5′ to the AU sequence (Fig. 4D and E).

Substitutions and nontemplated nucleotides in the imprecise recombinants discussed above consisted mainly of (90%) U residues and were preceded or followed by U residues (between 1 and 4 U residues). To test the importance of the presence of U residues on parental templates in the generation of these types of imprecise homologous recombinants, we made DIC4x-2 RNA2 (or DIC4x-6 RNA2) and PN-MA4x-11

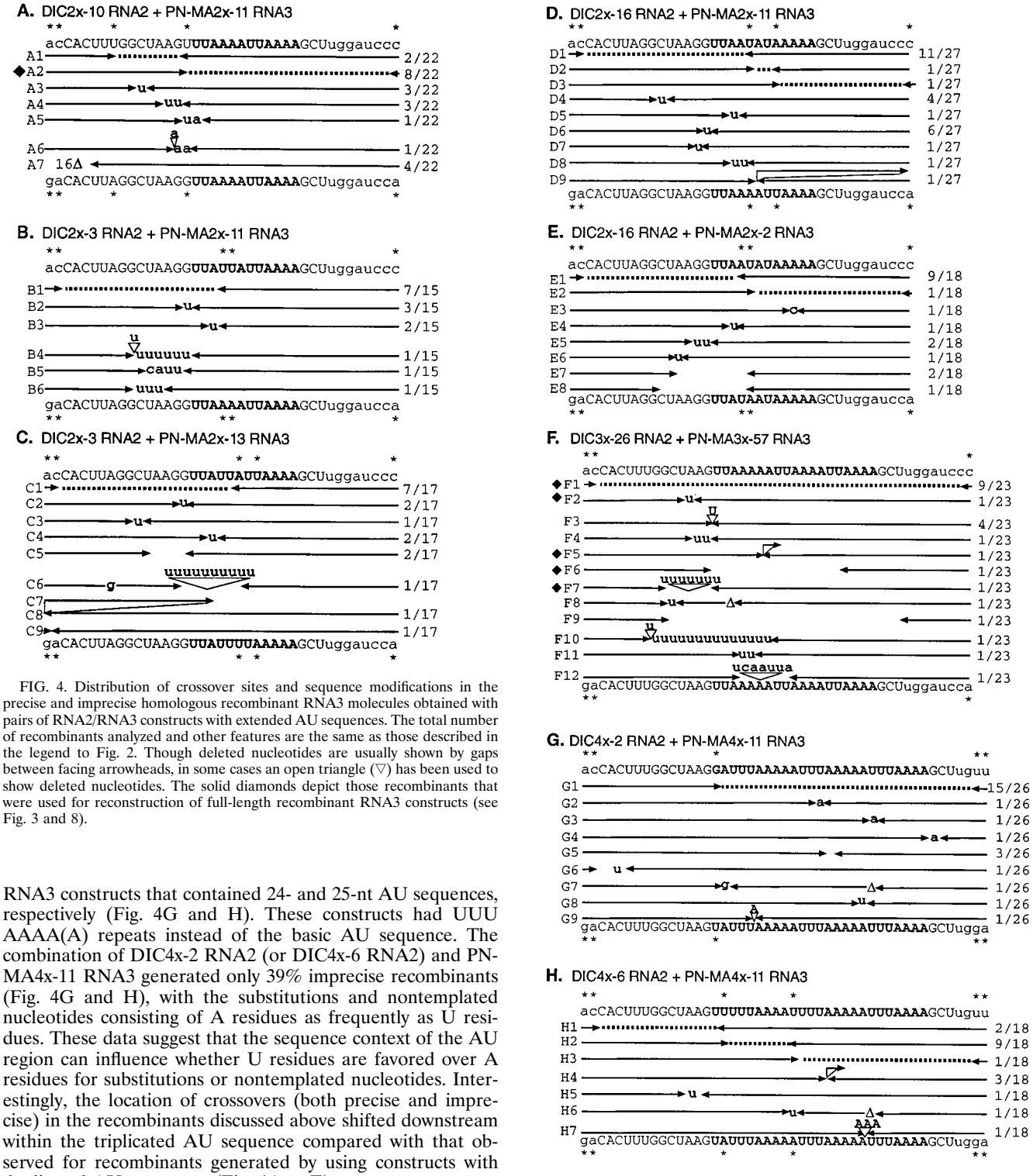


FIG. 4. Distribution of crossover sites and sequence modifications in the precise and imprecise homologous recombinant RNA3 molecules obtained with pairs of RNA2/RNA3 constructs with extended AU sequences. The total number of recombinants analyzed and other features are the same as those described in the legend to Fig. 2. Though deleted nucleotides are usually shown by gaps between facing arrowheads, in some cases an open triangle (▽) has been used to show deleted nucleotides. The solid diamonds depict those recombinants that were used for reconstruction of full-length recombinant RNA3 constructs (see Fig. 3 and 8).

RNA3 constructs that contained 24- and 25-nt AU sequences, respectively (Fig. 4G and H). These constructs had UUU AAAA(A) repeats instead of the basic AU sequence. The combination of DIC4x-2 RNA2 (or DIC4x-6 RNA2) and PN-MA4x-11 RNA3 generated only 39% imprecise recombinants (Fig. 4G and H), with the substitutions and nontemplated nucleotides consisting of A residues as frequently as U residues. These data suggest that the sequence context of the AU region can influence whether U residues are favored over A residues for substitutions or nontemplated nucleotides. Interestingly, the location of crossovers (both precise and imprecise) in the recombinants discussed above shifted downstream within the triplicated AU sequence compared with that observed for recombinants generated by using constructs with duplicated AU sequences (Fig. 4A to E).

The results of coinoculations with RNA2 and RNA3 constructs with different sizes of AU sequences are shown in Fig. 5. Specifically, coinoculation of DIC2x-14 RNA2 and PN-MA3x-57 RNA3 (Fig. 5C) generated imprecise recombinants with the highest frequency (86%). Coinoculations of DIC4x-6 RNA2 and PN-MA3x-57 RNA3 gave 65% imprecise recombinants (Fig. 5D), those of DIC3x-26 RNA2 and PN-MA4x-11 RNA3 gave 38% imprecise recombinants (Fig. 5A), and those of DIC4x-6 RNA2 and PN-MA2x-11 RNA3 gave 26% imprecise recombinants (Fig. 5B). Interestingly, a few identified imprecise recombinants had sequence modifications outside of the crossover region (e.g., rec-5D3, rec-5D6, and rec-5D14 [Fig. 5D]). Whether these recombinants arose from two separate crossover events or from a single complicated process is unknown.

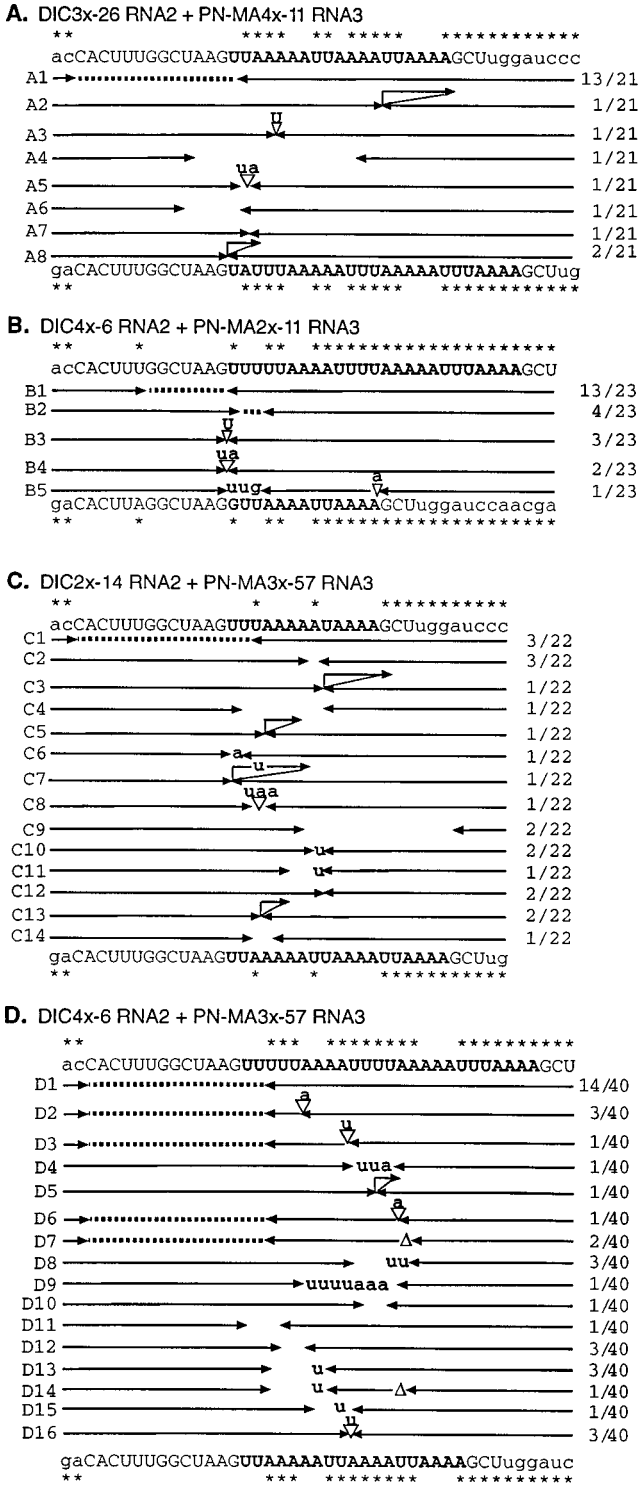


FIG. 5. Locations of crossover sites and sequence modifications in the precise and imprecise recombinant RNA3 molecules obtained with pairs of RNA2/RNA3 constructs with AU sequences of different lengths. The total number of recombinants analyzed and other features are the same as those described in the legends to Fig. 2 and 4.

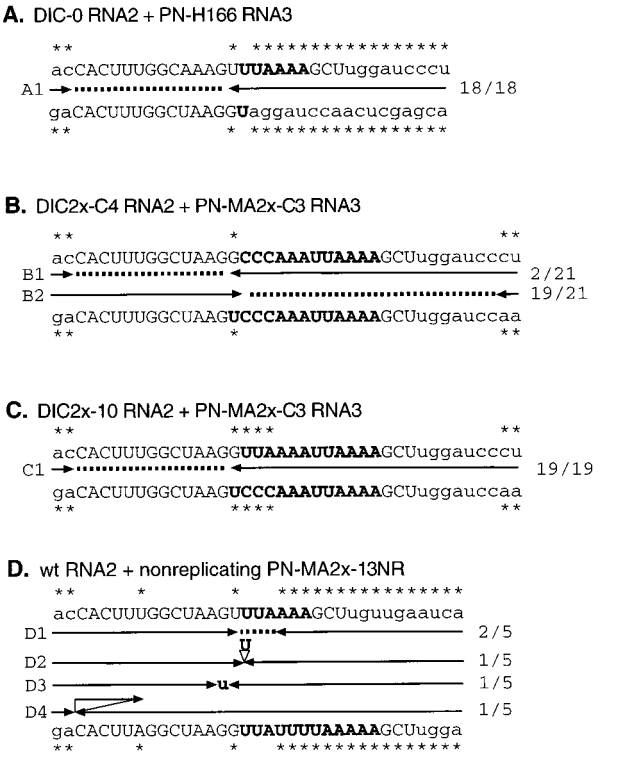


FIG. 6. Locations of crossover sites and sequence modifications in the precise and imprecise recombinant RNA3 molecules obtained with pairs of RNA2/RNA3 constructs that had AU sequences with RNA3 deleted (A), interrupted by C residues on both RNAs (B), interrupted by C residues in RNA3 (C), or obtained with a nonreplicating RNA3 construct (D). The total number of recombinants analyzed and other features are the same as those described in the legends to Fig. 2 and 4.

**Deletions of the AU sequence or the introduction of C residues into the AU sequence decrease the occurrence of imprecise recombinants.** To further test its role in homologous recombination, the AU region was removed from PN-H66. The resulting construct (PN-H166) had only the 5′ portion of region R′. When PN-H166 RNA3 was coinoculated with DIC-0 RNA2 and wt RNA1 on *C. quinoa* leaves, all 18 homologous recombinants were precise (Fig. 6A). When three A or U nucleotides in the 5′ portion of the duplicated AU sequences in DIC2x-10 RNA2 and PN-MA2x-11 RNA3, respectively, were replaced by C residues, coinfection of the resulting DIC2x-C4 RNA2 and PN-MA2x-C3 RNA3 with wt RNA1 produced only precise homologous recombinants (Fig. 6B). This demonstrated that the presence of three C residues close to the imprecise AU-rich crossover hot spot increased the accuracy of recombination.

An examination of the preferences in crossover events occurring with wt RNA2/PN-MA2x-2 RNA3 or DIC4x-6 RNA2/PN-MA4x-11 RNA3 combinations (Fig. 2D and 4G) revealed that one or two separated A (G) or U marker mutations located within the extended AU sequences in RNA2 and RNA3 did not interfere with the generation of precise and imprecise recombinants. However, two neighboring or three separated A (G) or U marker mutations (e.g., in DIC2x-3 RNA2/PN-MA2x-11 RNA3 infection [Fig. 4B]) caused a 5′ shift in the location of precise homologous crossovers, but the frequency and sites of imprecise crossovers were not altered.

In some cases (e.g., DIC2x-14 RNA2/PN-MA3x-57 RNA3 and DIC4x-6 RNA2/PN-MA3x-57 RNA3 infections [Fig. 5C

and D]), parental marker mutations were modified in progeny recombinants, indicating that these mutations might participate in crossover events. To test the effect of C marker mutations within the AU region on homologous recombination, construct PN-MA2x-C4 RNA3 was used in combination with wt RNA1 and DIC2x-10 RNA2 for infection. Analysis of 19 homologous recombinants revealed that all of them were precise (Fig. 6C). The region of crossovers was located upstream of the AU sequence. These experiments demonstrate that imprecise crossovers are sensitive to the presence of C, not A or U, marker mutations within the AU sequence (Fig. 5D).

**A nonreplicating RNA3 with an extended AU sequence generates imprecise homologous recombinants.** The replication of BMV RNAs produces both positive and negative daughter strands which are potentially available for recombination. To test if positive strands of RNA3 can participate in homologous recombination, a nonreplicating parental RNA3 construct was utilized (36). The construct designated PN-MA2x-11NR was derived by deleting the 3′ regions A and B and part of region C in PN-MA2x-11 (sequences between the *Spe*I and *Eco*RI sites [Fig. 1]) so that it lacked the negative-strand initiation promoter. Coinoculation of wt RNA1, wt RNA2, and PN-MA2x-11NR RNA3 induced a small number of local lesions. The sequencing of progeny RNA3 isolated from five local lesions revealed the accumulation of two precise and three imprecise recombinants (Fig. 6D). Two imprecise recombinants had a 1- or 7-nt insertion, and one had a G-to-U substitution right upstream of the AU sequence. These data demonstrate that positive strands of RNA3 can participate in recombination with a replication-competent RNA2.

**AU sequences are maintained in parental and recombinant progeny RNAs.** It is possible that some of the modifications discussed above were due to errors in RNA replication prior to recombination events. The stability of the region R′ in parental RNA2 or RNA3 progeny was determined by the sequencing of cDNA clones amplified by RT-PCR from total RNA extracts obtained from DIC2x-10 RNA2/PN-MA2x-11 RNA3, DIC2x-16 RNA2/PN-MA2x-11 RNA3, and wt RNA2/PN-MA 2x-13 RNA3 infections (Fig. 7). Primer pairs 1 and 3 and 1 and 2 were used to amplify RNA2 and RNA3 3′ sequences, respectively. As predicted, parental duplicated AU sequences and the 5′ portion of region R′ were maintained in RNA2 progeny; only 1 of 52 RNA2 samples (18 for DIC2x-10 RNA2 and 34 for DIC2x-16 RNA2) samples derived from separate local lesions contained an upstream U-to-C mutation (data not shown). On the other hand, the corresponding region of RNA3 was changed only in those local lesions that accumulated recombinants (Fig. 7); no sequence modifications were identified in the 40 samples (24 for PN-MA2x-11 RNA3 and 16 for PN-MA2x-13 RNA3) of nonrecombined RNA3 progeny. These results argue that the modifications found in imprecise homologous RNA3 recombinants were not generated prior to crossover events.

To test whether postrecombinational events can cause the observed sequence changes in progeny recombinant RNA3s, a full-length RNA3 construct containing a duplicated AU sequence found in recombinant rec-4A2 (Fig. 4A) was obtained. Coinoculation with wt RNA1 and DIC2x-10 RNA2 on *C. quinoa* leaves did not induce any changes within the AU sequence of rec-4A2 RNA3 in the 21 local lesions analyzed (data not shown). This finding suggests that the observed sequence changes in imprecise RNA3 progeny likely do not result from postrecombinational modifications.

The data for 113 separate samples also demonstrate that AU sequences can be amplified accurately by RT-PCR. This

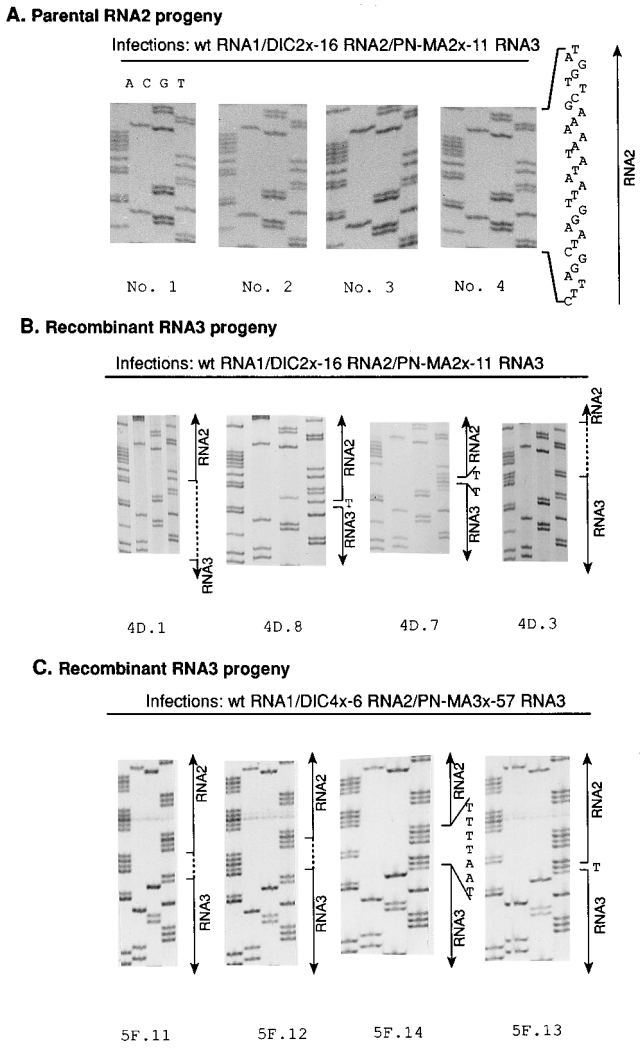


FIG. 7. Nucleotide sequences of the region R′ in the progeny of parental (nonrecombined) DIC2x-16 RNA2 (A) or recombinant RNA3s (B and C). Inoculations were carried out with a mixture wt RNA1, DIC2x-16 or DIC4x-6 RNA2, and PN-MA2x-11 or PN-MA3x-57 RNA3 (as shown above the sequences). The 3′ noncoding regions of RNA2 and RNA3 were amplified by RT-PCR with primer pairs 1 and 3 and 1 and 2, respectively (see Materials and Methods), from total RNA extracts obtained from separate local lesions of *C. quinoa*. The resulting RT-PCR products were cloned and sequenced as described in Materials and Methods. The region R′ sequences of four representative clones obtained from separate total RNA samples in each experiment are shown. The RNA2/RNA3 junction sites, nucleotide substitutions, and nontemplated nucleotides are shown next to sequencing gels. Dashed lines indicate ambiguous nucleotides that could be derived from either RNA2 or RNA3.

strongly suggests that the nucleotide changes shown in Fig. 2 and 4 to 6 were not due to errors in RT-PCR amplification.

**Growth characteristics of parental and recombinant RNAs.** Biased accumulation of precise and imprecise recombinants may result from the altered growth advantages (fitness) of parental RNA molecules. To test this, barley protoplasts were inoculated with a 1:1:1 molar mixture of wt RNA1 and mutant parental RNA2 and RNA3 (Fig. 8A). The levels of accumulation for all RNA2 and RNA3 variants in five combinations of RNA2s and RNA3s were comparable. Apparently, the modified sequences in the RNA2 and RNA3 constructs used did not change detectably the levels of RNA2 and RNA3 substrates available for recombination. Thus, the differences in the per-

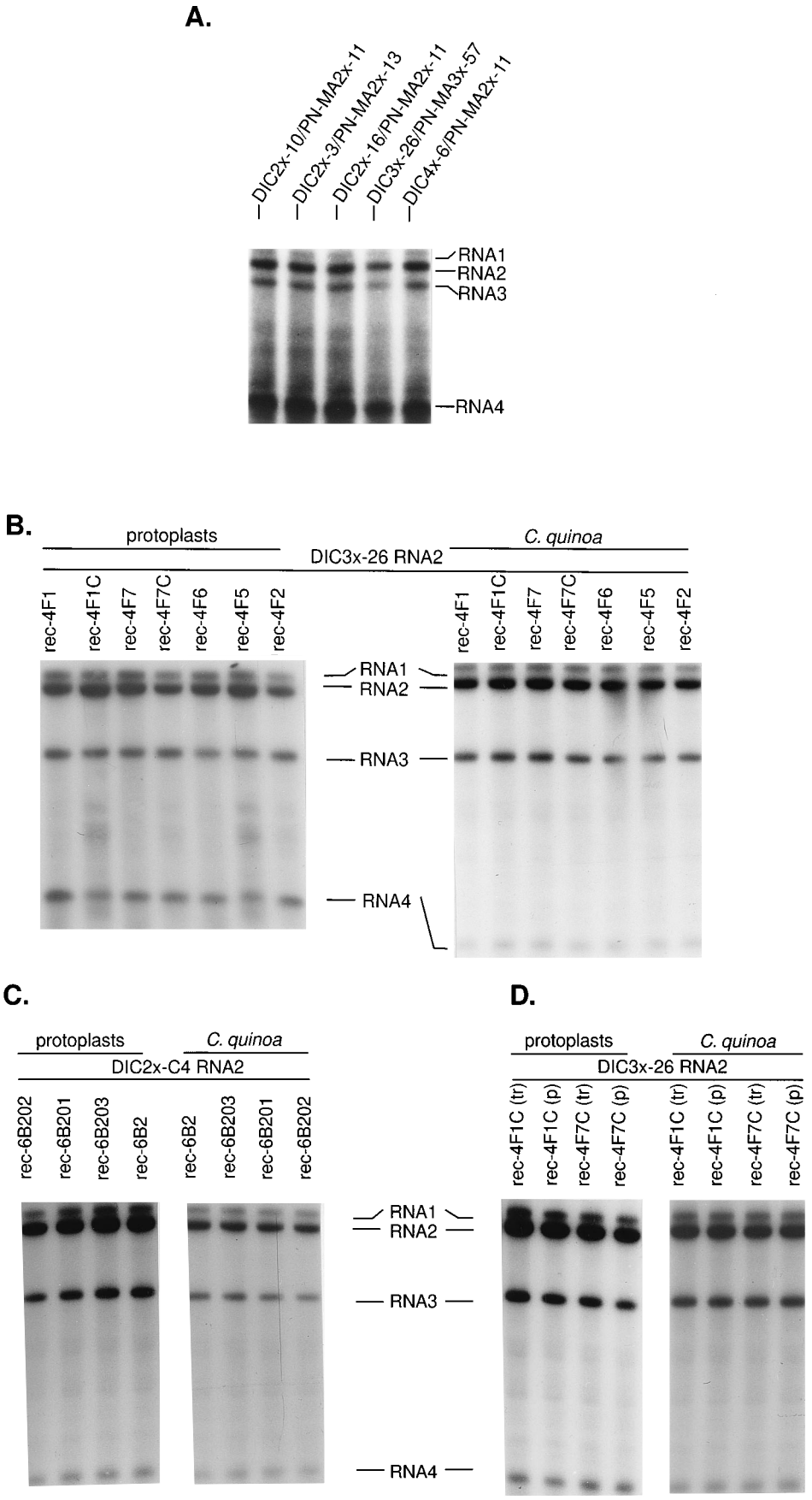
A.
DIC2x-10/PN-MA2x-11
DIC2x-3/PN-MA2x-13
DIC2x-16/PN-MA2x-11
DIC3x-26/PN-MA3x-57
DIC4x-6/PN-MA2x-11
RNA1
RNA2
RNA3
RNA4
B.
protoplasts
C. quinoa
DIC3x-26 RNA2
rec-4F1
rec-4F1C
rec-4F7
rec-4F7C
rec-4F6
rec-4F5
rec-4F2
RNA1
RNA2
RNA3
RNA4
C.
protoplasts
C. quinoa
DIC2x-C4 RNA2
rec-6B202
rec-6B201
rec-6B203
rec-6B2
rec-6B2
rec-6B203
rec-6B201
rec-6B202
RNA1
RNA2
RNA3
RNA4
D.
protoplasts
C. quinoa
DIC3x-26 RNA2
rec-4F1C (tr)
rec-4F1C (p)
rec-4F7C (tr)
rec-4F7C (p)
rec-4F1C (tr)
rec-4F1C (p)
rec-4F7C (tr)
rec-4F7C (p)

centages of precise and imprecise recombinants observed in this work cannot be due to altered selective advantages (or disadvantages) of parental RNA2s or RNA3s. Moreover, as shown above, the levels of a reconstructed recombinant RNA3 (rec-4A2) were the same in *C. quinoa* with four different parental RNA2s (Fig. 3B). We conclude that the altered sequences in region R′ in the parental RNA2 and RNA3 do not create new selective pressure on the emerged recombinant RNA3s.

Biased accumulation of recombinant RNA3 progeny can also result from altered growth advantages caused by mutations generated during or after crossover events. To test this possibility, we reconstructed the following five full-length cDNA clones of recombinant progeny RNA3s, each representing a separate de novo-generated recombinant molecule: one precise recombinant (rec-4F1) and four imprecise recombinants with either a mismatch (rec-4F2), 15-nt deletion (rec-4F6), 2-nt insertion (rec-4F5), or 7 added nontemplated U residues followed by 5 deleted nucleotides (rec-4F7). The entire transferred regions (approximately 160 nt and located between *Xba*I and *Bam*HI sites [Fig. 1]) in these recombinants have been sequenced to exclude additional RT-PCR-derived mutations. In addition, one precise recombinant RNA3 (rec-4F1C) and one imprecise recombinant RNA3 (rec-4F7C) were regenerated by in vitro mutagenesis and cloning to make sure that the 3′ noncoding region is the only genetically altered region in the entire RNA3 sequence. Barley protoplasts and *C. quinoa* plants were coinoculated with wt RNA1, DIC3x-26 RNA2, and reconstructed recombinant RNA3s. Viral RNA levels were monitored by Northern blot analysis. We found that all of the reconstructed recombinant RNA3s accumulated to comparable levels in both systems (Fig. 8B). These data demonstrate that very different types of precise and imprecise homologous RNA3 recombinants can grow to similar levels, arguing that they would have been detected if they had been generated during infection.

Another possible influence on the recombinant profile is that mutations elsewhere in the RNA genome contribute to the growth advantage of recombinants. These putative mutations are expected to become fixed in the population. To test this idea, we compared the growth characteristics of one precise recombinant (rec-4F1C) and one imprecise recombinant (rec-4F7C) constructed by cloning. Barley protoplasts and *C. quinoa* plants were inoculated either with in vitro-transcribed RNAs or with total RNA extracts from transcript-inoculated protoplasts or plants (first passage of the virus in both systems), respectively. One can expect secondary mutations accumulating in the recombinant RNA genome to be manifested through an increased growth advantage for passaged RNAs compared with transcript-derived RNAs. The accumulations of transcript-derived and passaged RNAs were similar for both recombinants in barley protoplasts and *C. quinoa* plants (Fig. 8D). This observation suggests that mutations accumulating in the RNA genome, if any, did not detectably increase the fitness of progeny recombinants in this system.

If selection pressure among recombinant progeny is responsible for the recombination profiles observed, this factor should be the most obvious one in wt RNA1/DIC2x-C4 RNA2/PN-MA2x-C3 RNA3 infections, in which only precise homologous recombinants were detected (Fig. 6B). They should give the most biased accumulation of recombinant RNA3 progeny. To test whether imprecise homologous recombinants can grow well in this particular system, three imprecise recombinants that resembled those observed in other experiments (e.g., the recombinants shown in Fig. 4A to F) were made by in vitro mutagenesis and cloning. One of these constructed imprecise recombinants had two nontemplated U residues within its AU sequence (rec-6B203), another had a single C-to-U substitution (rec-6B201), and the third one contained four nucleotide substitutions (rec-6B202) in region R′. The accumulation of these recombinant RNA3s was tested separately in the presence of wt RNA1 and DIC2x-C4 RNA2 in barley protoplasts and *C. quinoa* plants. All three imprecise homologous recombinant RNA3s grew as well as the reconstructed precise recombinant RNA3 (rec-6B2) both in barley protoplasts and in *C. quinoa* plants (Fig. 8C). These results further support the idea that imprecise homologous recombinants would have grown well if they had been formed.

## DISCUSSION

In this study, we have demonstrated that the presence of AU-rich sequences in recombining RNAs can facilitate the generation of imprecise homologous recombinants in BMV. Indeed, the lack of these AU sequences (Fig. 6A) or the replacement of portions of AU sequences with C residues (Fig. 6B) in RNA3 templates strongly increased the accuracy of homologous crossovers. In contrast, expanding the AU sequence in one or both recombining RNAs increased the incidence of imprecise recombinants. In addition to length, the actual nucleotide order of the AU sequences influences the accuracy of crossovers.

It is unlikely that the observed differences in the profiles of precise and imprecise recombinant RNA3s are due to altered selection pressure among different combinations of parental RNAs, as no differences in the accumulation levels of parental RNA2s or RNA3s were observed in barley protoplasts. In addition, different recombinant RNA3s accumulated to similar levels in both protoplasts and *C. quinoa* plants. Apparently, various sequence modifications in region R′ do not change the postrecombination selection among recombinants in these hosts. Therefore, the recombinant profiles shown in Fig. 2 and 4 to 6 most likely reflect the frequencies of the generation of these recombinants.

Frequent generation of imprecise homologous recombinants was observed between satellite RNA C and RNA D in TCV infections (13, 14). However, unlike in BMV, no precise homologous RNA C/RNA D recombinants have been identified. The crossover junctions cluster at promoter-like sequences (motifs) on RNA C, while in satellite RNA D, the junctions are near the 3′ end. In contrast, BMV recombinant junctions occur within a common 3′ region (R′) that neither functions as a promoter of BMV RNA synthesis nor is important in RNA accumulation (28, 42). In TCV, a stem-loop structure in RNA C is important for recombination (14); the role of secondary structures in recombination is not clear for BMV, as all of the modifications tested here were introduced into the loop part of a hairpin in region R′ (data not shown). As in BMV, imprecise

FIG. 8. Analysis of the accumulation levels of various reconstructed and engineered RNA2 and RNA3 mutants in barley protoplasts and whole plants, as determined by Northern blotting. (A) Accumulation levels of parental RNA2s and RNA3s in barley protoplasts; (B and C) Growth levels of various reconstructed and engineered RNA3s in barley protoplasts and *C. quinoa* plants; (D) RNA samples obtained from separate local lesions induced by either in vitro-transcribed RNA (tr) or total RNA derived from transcript-inoculated plants (first passage [p]). The inoculation of barley protoplasts and whole plants, total RNA extraction, and Northern blotting are the same as those described in the legend to Fig. 3.

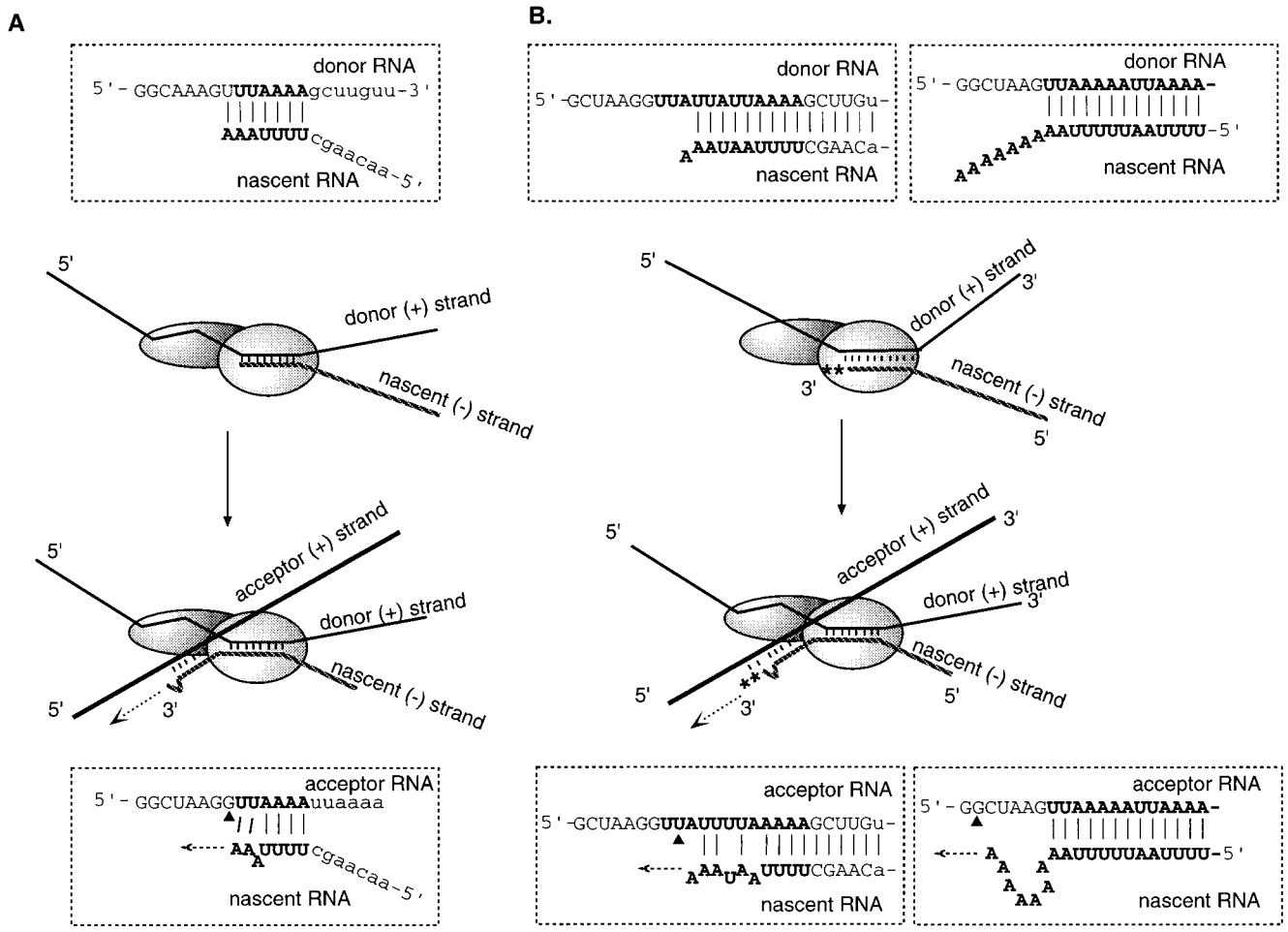


FIG. 9. Diagrammatic representations of processive template switching models explaining the generation of imprecise homologous recombinants. (A) The replicase pauses and then marches back on the donor strand so that the very 3′ end of the nascent strand disengages from the template strand. The released 3′ end of the nascent RNA can then misalign at the complementary region of the acceptor strand, with subsequent resumption of chain elongation by the replicase on the acceptor strand. This leads to the formation of type I imprecise recombinant RNA3s. An example of misalignment leading to the formation of rec-2B4 (Fig. 2B) is shown in the box. The donor and acceptor sequences are shown in positive sense, while the nascent RNA is displayed in negative sense. The opposite scenario with the participation of negative-stranded donor and acceptor and positive-sense nascent RNAs is also possible (not shown). A filled triangle points to the first nucleotide derived from the acceptor RNA. (B) The replicase pauses on the donor template and introduces nontemplated nucleotides (mainly A or U residues) to the 3′ end of the nascent strand. Alternatively, nucleotide misincorporation during chain elongation causes the replicase to pause on the donor template. Then, misalignment of the free 3′ end of the nascent strand at the complementary region of the acceptor strand leads to the formation of type II and III imprecise recombinant RNA3s. Two examples of RNA3 recombinants with either a nucleotide substitution (rec-4C4) or nontemplated nucleotides (rec-4F7) at the crossover sites are shown in the left and right boxes, respectively.

TCV recombinants have nontemplated nucleotide insertions (mainly U residues on the positive strand) at the crossover sites (13, 14). Though the crossover regions of the two satellite RNAs of TCV are not particularly AU rich, there is a 6-nt AU sequence (interrupted by one G) that includes a recombination hot spot in satellite RNA C.

At least the majority of the observed sequence modifications in imprecise BMV recombinants must have happened during crossover events. This conclusion is based on the fact that these sequence modifications occur between marker mutations, within or immediately 5′ to the active AU sequence. In addition, AU sequences are maintained in both parental and recombinant RNA molecules during infection, and RT-PCRs are shown not to contribute to these modifications.

The identified imprecise homologous recombinants can be divided into three groups. The first type contains sequence insertions (duplications) or deletions within the homologous region (e.g., rec-4C5, rec-4F5, and rec-4F6 [Fig. 4C and F]) that could be entirely derived from parental molecules. In contrast, the second type has nucleotide substitutions (mainly U residues and, less frequently, A residues), that are not present in parental molecules (e.g., rec-4C2 and rec-4C4 [Fig. 4C]). The third type contains nontemplated nucleotides (also mainly U residues) within the crossover region (e.g., rec-4C6 and rec-4F10 [Fig. 4C and F]). It is important that several imprecise recombinants can be placed in more than one of these groups because of the presence of ambiguous sequences at the crossover sites (Fig. 2 and 4 to 6 [capital letters]).

Both the nonprocessive and processive models of homologous recombination have been postulated (22, 29, 37). According to these models, we predict that BMV replicase can pause within or close to the AU region because of the difficulties in reading through AU-rich sequences, a nucleotide misincorporation within the slippery sequence, temporal depletion of the UTP pool (less likely the ATP pool), or a break on the template that might occur within the less structured AU sequence.

After pausing, the replicase-nascent RNA complex can either dissociate from the primary RNA template and reassociate on another template (nonprocessive model) or occasionally retract on the primary template, exposing a short nascent strand sequence (22, 37) that can rehybridize to the new template. Both models predict that imprecise (type I) homologous recombinants emerge when the very 3′ end of the nascent strand misanneals to the complementary sequence on the acceptor strand (Fig. 9A). Accordingly, most type I imprecise crossovers occur at AU-rich sequences because of the lower energy levels of AU base pairing (19) and the possibility of alternate pairings.

Figure 9B shows another model that explains the generation of type II and III imprecise recombinants. Here we propose that the pausing replicase can misincorporate or add nontemplated nucleotides during or right before crossover events. Certainly, the AU sequence is more efficient in releasing the 3′ end of the nascent strand from the donor strand than is a GC-rich sequence. Furthermore, the AU sequence can be slippery for the BMV replicase and cause the addition of nontemplated nucleotides. Reiterative copying of one or a few adjacent nucleotides (slippage) has been described for several viral and nonviral polymerases, including DNA-dependent RNA polymerases and RNA-dependent RNA polymerases (7, 13, 20, 32, 38, 48). In BMV, the variable length of an intercistronic oligo(A) tract in RNA3 (2) suggests that BMV replicase is capable of stuttering. The nontemplated nucleotides present at the 3′ end of the nascent strand could cause misalignment to the complementary region of the acceptor strand (Fig. 9B). The subsequent resumption of chain elongation would then occur from the unpaired (or mispaired) 3′ end of the nascent strand (Fig. 9B). One might speculate that nucleotide misincorporation or nontemplated addition of nucleotides would not only cause misannealing but also promote crossover events by forcing the replicase to pause. It is also equally possible that nucleotide addition and misincorporation are only the consequences of crossover events, i.e., they would occur during the process of template switching as the polymerase pauses on the donor template.

Crossovers that occur during either positive- or negative-strand synthesis can lead to the generation of the observed recombinants. The models shown in Fig. 9A and B propose that misannealing occurs between the negative nascent and positive acceptor RNA strands. This is supported by the results of experiments with a nonreplicating RNA3 (PN-MA2x-13NR [Fig. 6D]) that did not contain a negative-strand initiation promoter and produced both precise and imprecise homologous recombinants. However, the opposite scenario of recombination events occurring during plus-strand synthesis is also possible in infections in which both recombining RNAs are replication competent. This needs further experimental conformation.

Our models suggest direct RNA-RNA hybridization between the nascent and the acceptor strands within or immediately 5′ to the common AU sequences. However, protein-protein or protein-RNA interactions similar to those proposed to describe leader-mRNA fusions during coronavirus transcription (51, 56) may also influence the selection of crossover sites. However, in the BMV system it is not so obvious as it is in coronaviruses where a promoter sequence on the RNA template at the fusion (crossover) site can potentially facilitate the positioning of putative transcription factors or complexes. The R′ region of BMV RNA3 has no demonstrated promoter function (28, 42). In fact, coronavirus transcription and consequently the association of transcription or other protein factors are adapted, and likely required, to produce abundant amounts of subgenomic RNAs during the virus life cycle. It remains to be seen whether protein-protein or RNA-protein interactions influence the selection of crossover sites in BMV.

Similar to previously described homologous recombination events in BMV (37), imprecise crossovers required high levels of sequence identity within the common AU region. The introduction of three C mutations into the 5′ portion of the AU sequence in PN-MA2x-C3 RNA3 (Fig. 6C) eliminated the appearance of imprecise recombinants and caused a 5′ shift in the location of precise crossover sites. The introduction of A or U marker mutations affected imprecise crossovers to a lesser extent. This could have been because the nascent RNA strands contain nontemplated A or U nucleotides (as described above) which can be accidentally complementary with the introduced A or U markers, but not C markers, reducing the potential for misalignment. Actually, depending on the recombining parental RNA sequences and on the site(s) of the A or U markers, these mutations can be either preserved or eliminated during imprecise crossovers.

Homologous recombination processes differ from the heteroduplex-mediated nonhomologous processes previously reported for BMV (36). For the latter, the sites of crossovers were distributed between noncorresponding nucleotides at one side of a heteroduplex formed between recombining RNAs. Perfect heteroduplexes of longer than 20 bp were required to support efficient recombination events (36). Though imperfect heteroduplexes can be formed between R′ region sequences of RNA2 and RNA3 constructs (data not shown), it is unlikely that such energetically weak, mismatched heteroduplexes can promote the observed efficient crosses. Our results for imprecise recombinants open new experimental opportunities toward understanding the role of different sequences in RNA-RNA recombination not only in BMV but in other RNA viruses as well.

## ACKNOWLEDGMENTS

We thank A. Ball, M. Figlerowicz, C. Ogiela, J. Pogany, D. Rochon, and A. White for comments and discussions.

This work was supported by grants from the National Institute for Allergy and Infectious Diseases (RO1 AI26769) and National Science Foundation (MCB-9305389) and by the Plant Molecular Biology Center at Northern Illinois University.

## REFERENCES

1. **Ahlquist, P.** 1992. Bromovirus RNA replication and transcription. Curr. Opin. Genet. Dev. **2:**71–76.
2. **Ahlquist, P., R. Dasgupta, and P. Kaesberg.** 1984. Nucleotide sequence of the brome mosaic virus genome and its implications for viral replication. J. Mol. Biol. **172:**369–383.
3. **Allison, R. F., M. Janda, and P. Ahlquist.** 1989. Sequence of cowpea chlorotic mottle virus RNAs 2 and 3 and evidence of a recombination event during bromovirus evolution. Virology **172:**321–330.
4. **Allison, R. F., G. Thompson, and P. Ahlquist.** 1990. Regeneration of a functional RNA virus genome by recombination between deletion mutants and requirement for cowpea chlorotic mottle virus 3a and coat genes for systemic infection. Proc. Natl. Acad. Sci. USA **87:**1820–1824.
5. **Beck, D. L., and W. O. Dawson.** 1990. Deletion of repeated sequences from tobacco mosaic virus mutants with two coat protein genes. Virology **177:**462–469.
6. **Bergmann, M., A. Garcia-Sastre, and P. Palese.** 1992. Transfection-mediated recombination of influenza A virus. J. Virol. **66:**7576–7580.
7. **Bertholet, C., E. van Meir, B. ten Heggeler-Bordier, and R. Wittek.** 1987. Vaccinia virus produces late mRNAs by discontinuous synthesis. Cell **50:**153–162.
8. **Biebricher, C. K., and R. Luce.** 1992. In vitro recombination and terminal elongation of RNA by Qβ replicase. EMBO J. **11:**5129–5135.
9. **Bujarski, J. J., and A. M. Dzianott.** 1991. Generation and analysis of nonhomologous RNA-RNA recombinants in brome mosaic virus: sequence complementarities at crossover sites. J. Virol. **65:**4153–4159.
10. **Bujarski, J. J., and P. Kaesberg.** 1986. Genetic recombination between RNA components of a multipartite plant virus. Nature (London) **321:**528–531.

11. **Bujarski, J. J., and P. D. Nagy.** 1994. Genetic RNA-RNA recombination in positive-stranded RNA viruses of plants, p. 1–24. *In* J. Paszkowski (ed.), Homologous recombination in plants. Kluwer Academic Publisher, Dordrecht, The Netherlands.
12. **Bujarski, J. J., P. D. Nagy, and S. Flasinski.** 1994. Molecular studies of genetic RNA-RNA recombination in brome mosaic virus. Adv. Virus Res. **43:**275–302.
13. **Cascone, P. J., C. D. Carpenter, X. H. Li, and A. E. Simon.** 1990. Recombination between satellite RNAs of turnip crinkle virus. EMBO J. **9:**1709–1715.
14. **Cascone, P. J., T. F. Haydar, and A. E. Simon.** 1993. Sequences and structures required for recombination between virus-associated RNAs. Science **260:**801–805.
15. **Dolja, V. V., and J. C. Carrington.** 1992. Evolution of positive-strand RNA viruses. Semin. Virol. **3:**315–326.
16. **Goldbach, R., O. Le Gall, and J. Wellink.** 1991. Alpha-like viruses in plants. Semin. Virol. **2:**19–25.
17. **Greene, A. E., and R. F. Allison.** 1994. Recombination between viral RNA and transgenic plant transcripts. Science **263:**1423–1425.
18. **Ishikawa, M., P. Kroner, P. Ahlquist, and T. Meshi.** 1991. Biological activities of hybrid RNAs generated by 3′-end exchanges between tobacco mosaic and brome mosaic viruses. J. Virol. **65:**3451–3459.
19. **Jacobsen, A. B., L. Good, J. Simonetti, and M. Zuker.** 1984. Some simple computational methods to improve the folding of large RNAs. Nucleic Acids Res. **12:**45–52.
20. **Jacques, J. P., S. Hausmann, and D. Kolakofsky.** 1994. Paramyxovirus mRNA editing leads to G deletions as well as insertions. EMBO J. **13:**5496–5503.
21. **Janda, M., R. French, and P. Ahlquist.** 1987. High efficiency T7 polymerase synthesis of infectious RNA from cloned brome mosaic virus cDNA and effects of 5′ extensions of transcript infectivity. Virology **158:**259–262.
22. **Jarvis, T. C., and K. Kirkegaard.** 1991. The polymerase in its labyrinth: mechanisms and implications of RNA recombination. Trends Genet. **7:**186–191.
23. **Jarvis, T. C., and K. Kirkegaard.** 1992. Poliovirus RNA recombination: mechanistic studies in the absence of selection. EMBO J. **11:**3135–3145.
24. **King, A. M. Q.** 1988. Genetic recombination in positive strand RNA viruses, p. 149–185. *In* E. Domingo, J. J. Holland, and P. Ahlquist (ed.), RNA genetics, vol. 2. CRC Press, Boca Raton, Fla.
25. **Kirkegaard, K., and D. Baltimore.** 1986. The mechanism of RNA recombination in poliovirus. Cell **47:**433–443.
26. **Kroner, P., D. Richards, P. Traynor, and P. Ahlquist.** 1989. Defined mutations in a small region of the brome mosaic virus 2a gene cause diverse temperature-sensitive RNA replication phenotypes. J. Virol. **63:**5302–5309.
27. **Kuge, S., I. Saito, and A. Nomoto.** 1986. Primary structure of poliovirus defective-interfering particule genomes and possible generation mechanisms of the particules. J. Mol. Biol. **192:**473–487.
28. **Lahser, F. C., L. E. Marsh, and T. C. Hall.** 1993. Contributions of the brome mosaic virus RNA-3 3′-nontranslated region to replication and translation. J. Virol. **67:**3295–3303.
29. **Lai, M. M. C.** 1992. RNA recombination in animal and plant viruses. Microbiol. Rev. **56:**61–79.
30. **Lane, L. C.** 1977. Brome mosaic virus. CMI/AAB descriptions of plant viruses no. 180. Commonwealth Agricultural Bureaux, Farnham Royal, Slough, England.
31. **Li, Y., and L. A. Ball.** 1993. Nonhomologous RNA recombination during negative-strand synthesis of flock house virus RNA. J. Virol. **67:**3854–3860.
32. **Luo, G., W. Luytjes, M. Enami, and P. Palese.** 1991. The polyadenylation signal of influenza virus RNA involves a stretch of uridines followed by the RNA duplex of the panhandle structure. J. Virol. **65:**2861–2867.
33. **Makino, S., J. G. Keck, S. A. Stohlman, and M. M. C. Lai.** 1986. High-frequency RNA recombination of murine coronaviruses. J. Virol. **57:**729–737.
34. **Marsh, L. E., G. P. Pogue, C. C. Huntley, and T. C. Hall.** 1991. Insight to replication strategies and evolution of (+) strand RNA viruses provided by brome mosaic virus. Oxf. Surv. Plant Mol. Cell Biol. **7:**297–334.
35. **Nagy, P. D., and J. J. Bujarski.** 1992. Genetic recombination in brome mosaic virus: effect of sequence and replication of RNA on accumulation of recombinants. J. Virol. **66:**6824–6828.
36. **Nagy, P. D., and J. J. Bujarski.** 1993. Targeting the site of RNA-RNA recombination in brome mosaic virus with antisense sequences. Proc. Natl. Acad. Sci. USA **90:**6390–6394.
37. **Nagy, P. D., and J. J. Bujarski.** 1995. Efficient system of homologous RNA recombination in brome mosaic virus: sequence and structure requirements and accuracy of crossovers. J. Virol. **69:**131–140.
38. **Nagy, P. D., A. Dzianott, P. Ahlquist, and J. J. Bujarski.** 1995. Mutations in the helicase-like domain of protein 1a alter the sites of RNA-RNA recombination in brome mosaic virus. J. Virol. **69:**2547–2556.
39. **Onodera, S., X. Qiao, P. Gottlieb, J. Strassman, M. Frilander, and L. Mindich.** 1993. RNA structure and heterologous recombination in the double-stranded RNA bacteriophage ϕ6. J. Virol. **67:**4914–4922.
40. **Palasingam, K., and P. N. Shaklee.** 1992. Reversion of Qβ RNA phage mutants by homologous RNA recombination. J. Virol. **66:**2435–2442.
41. **Raffo, A. J., and W. O. Dawson.** 1991. Construction of tobacco mosaic virus subgenomic replicons that are replicated and spread systemically in tobacco plants. Virology **184:**277–289.
42. **Rao, A. L. N., and T. C. Hall.** 1990. Requirement for a viral *trans*-acting factor encoded by brome mosaic virus RNA-2 provides strong selection in vivo for functional recombinants. J. Virol. **64:**2437–2441.
43. **Rao, A. L. N., and T. C. Hall.** 1993. Recombination and polymerase error facilitate restoration of infectivity in brome mosaic virus. J. Virol. **67:**969–979.
44. **Rao, A. L. N., B. P. Sullivan, and T. C. Hall.** 1990. Use of *Chenopodium hybridum* facilitates isolation of brome mosaic virus RNA recombinants. J. Gen. Virol. **71:**1403–1407.
45. **Romanova, L. I., V. M. Blinov, E. A. Tolskaya, E. G. Viktorova, M. S. Kolesnikova, E. A. Guseva, and V. I. Agol.** 1986. The primary structure of crossover regions of intertypic poliovirus recombinants: a model of recombination between RNA genomes. Virology **155:**202–213.
46. **Sambrook, J., E. F. Fritsch, and T. Maniatis.** 1989. Molecular cloning: a laboratory manual, 2nd ed. Cold Spring Harbor Laboratory, Cold Spring Harbor, N.Y.
47. **Strauss, J. H., and E. G. Strauss.** 1988. Evolution of RNA viruses. Annu. Rev. Microbiol. **42:**657–683.
48. **Thomas, S. M., R. A. Lamb, and R. G. Paterson.** 1988. Two mRNAs that differ by two nontemplated nucleotides encode the amino coterminal proteins P and V of the paramyxovirus SV5. Cell **54:**891–902.
49. **Tolskaya, E. A., L. I. Romanova, V. M. Blinov, E. G. Viktorova, A. N. Sinyakov, M. S. Kolesnikova, and V. I. Agol.** 1987. Studies on the recombination between RNA genomes of poliovirus: the primary structure and nonrandom distribution of crossover regions in the genomes of intertypic poliovirus recombinants. Virology **161:**54–61.
50. **Van der Kuyl, A. C., L. Neeleman, and J. F. Bol.** 1991. Complementation and recombination between alfalfa mosaic virus RNA3 mutants in tobacco plants. Virology **183:**731–738.
51. **van der Most, R. G., R. J. de Groot, and W. J. M. Spaan.** 1994. Subgenomic RNA synthesis directed by a synthetic defective interfering RNA of mouse hepatitis virus: a study of coronavirus transcription initiation. J. Virol. **68:**3656–3666.
52. **Van der Most, R. G., L. Heijnen, W. J. M. Spaan, and R. J. de Groot.** 1992. Homologous RNA recombination allows efficient introduction of site-specific mutations into the genome of coronavirus MHV-A59 via synthetic co-replicating RNAs. Nucleic Acids Res. **20:**3375–3381.
53. **Weiss, B. G., and S. Schlesinger.** 1991. Recombination between Sindbis virus RNAs. J. Virol. **65:**4017–4025.
54. **White, K. A., and T. J. Morris.** 1994. Nonhomologous RNA recombination in tombusviruses: generation and evolution of defective interfering RNAs by stepwise deletions. J. Virol. **68:**14–24.
55. **White, K. A., and T. J. Morris.** 1994. Recombination between defective tombusvirus RNAs generates functional hybrid genomes. Proc. Natl. Acad. Sci. USA **91:**3642–3646.
56. **Zhang, X., and M. M. C. Lai.** 1994. Unusual heterogeneity of leader-mRNA fusion in a murine coronavirus: implications for the mechanism of RNA transcription and recombination. J. Virol. **68:**6626–6633.
57. **Zimmern, D.** 1988. Evolution of RNA viruses, p. 211–240. *In* E. Domingo, J. J. Holland, and P. Ahlquist (ed.), RNA genetics, vol. 2. CRC Press, Boca Raton, Fla.